Epoxy Resin doped with Coumarin 6: example of accessible luminescent collectors

Matteo Sottile,[a] Giovanni Tomei,[a] Silvia Borsacchi,[b,c] Francesca Martini,[a,b] Marco Geppi,[a,b,c] Giacomo Ruggeri,[a,b] Andrea Pucci[a,b]

[a]Dipartimento di Chimica e Chimica Industriale, Università di Pisa, Via G. Moruzzi 13, 56124 Pisa, Italy
[b]INSTM, UdR Pisa, Via G. Moruzzi 13, 56124 Pisa Italy
[c]ICCOM-CNR, U.O.S. di Pisa, via G. Moruzzi 1, 56124 Pisa, Italy

Corresponding author:

Andrea Pucci, Dipartimento di Chimica e Chimica Industriale, Università di Pisa, Pisa, Italy; e-mail: andrea.pucci@unipi.it

Abstract

We report on the preparation of luminescent collectors based on epoxy resins containing Coumarin 6 as fluorescent dye. Fluorescent epoxy slabs were obtained by carefully mixing from 60 to 150 ppm of the fluorophore with bisphenol A diglycidyl ether and 4,4'-methylenebis(2-methylcyclohexylamine) as curing agent. Spectroscopic (FT-IR, solid-state NMR, Raman) investigations and calorimetric analysis evidence the success of the preparation procedure in terms of slab homogeneity, fluorophore dispersibility and its role in promoting the crosslinking extent. The concentrating ability and the derived optical efficiencies of the epoxy-based collectors are determined with a properly designed set-up and result greater (~10%) than that of poly(methyl methacrylate) concentrators with the same fluorophore and geometry. Optical efficiencies as high as 7.4% are obtained and enable the potential use of epoxy resins as bulk thermosetting materials for solar collectors.

1. Introduction

Fluorescent collectors are a promising path to cost-effective photovoltaic (PV) technologies thanks to several advantages: low weight, ability to work well with diffuse light and no needs of sun tracking or cooling apparatuses.[1] Moreover, these systems have recently received great impulse thanks to the modern building architectures that have inspired PV application of colourful windows.[2, 3] The building-integrated PV market is actually set to steadily increase promoted by the European Energy Performance of Buildings Directive 2010/31/EU, which states that each new building should be made 'nearly zero energy' from 2020 onwards.[4] Notably, fluorescent collectors, known also as luminescent solar concentrators (LSCs), are slabs of transparent material doped with a fluorophore.[5] The refractive index of the host higher than the environment traps a fraction of the emitted photons by means of total internal reflection. Photons are then collected at the edges of the slab to produce electric power by means of PV cells. The use of commodity plastics and consolidated industrial processes offer encouraging means to include solar energy to the built environment. The research on LSC-PV systems has been focusing on high power conversion efficiencies (PCE)[6-13] by selecting even more efficient organic or inorganic fluorophores[14-18] or by enhancing the spectral absorption window of collectors, therefore increasing the number of available photons.[7, 19-23] Sloff described a stacked device with PCE of 7.1%, which is, at best of our knowledge, the highest value ever reported for LSC-PV systems.[24] Conventional fluorescent collectors are made of visible transparent plates or films of poly(methyl methacrylate) (PMMA). However, PMMA is affected by two important drawbacks: the first resides in an evident shrinkage during polymerization and moulding,[25] which induces additional steps in LSC realization; the second consists in the apparent NIR absorption due to overtones of C-H vibration bands of PMMA (Figure S1),[26] thus limiting solar concentration in this spectral region.

This study proposes to investigate epoxy resins as accessible thermosetting fluorescent collectors, aimed to help the distribution of PV technology in the modern building architectures. The worldwide market for epoxy resins is slated to reach 3.03 million tons by the year 2017.[27]

Demand for epoxy resins is enormous due to their low cost and solid performance in both interior and exterior applications. Epoxies are the most versatile and utilised materials for high-tech applications. The most widely used epoxies are based on diglycidyl ethers of bisphenol A and epichlorohydrin (Figure 1), which provide fast monomer conversions and NIR transmittance (Figure S1).[28, 29] In the scenario of a sustainable economy, epoxy resins, and thermoset materials in general, can be efficiently obtained from renewable resources and ecofriendly processes[30, 31]. Moreover, epoxy resins and thermosets can be also rendered reworkable by using a series of thermally cleavable linkages.[32, 33]

Fluorophore doped epoxies have been already utilised in optical waveguides, light emitting diodes (LEDs)[34] and chromogenic materials[35] and attempts for polymer photostability under light exposure have been successfully made since years.[36] As far as LSC applications are concerned, they can offer outstanding physical attributes, including high physical strength, excellent adhesion to a variety of substrates, broad temperature resistance and the ability to cure in sections with controlled thickness. Moreover, epoxy resins possess superior properties with respect to PMMA such as minimal shrinkage during curing, good resistance to moisture, solvents and chemical attacks.[37] By contrast, the thermoset nature of epoxy resins might lead to a reduced reservoir of compatible fluorophores. Nevertheless, only a few examples have been reported so far for the preparation of epoxy-based fluorescent collectors.[38-40] Notably, this study examines the use of high quantum yield (QY) fluorophores such as Coumarin 6 (QY = 97-99%) [41] and Lumogen Red F350 (QY = 95-96%) [42] in epoxy-based fluorescent slabs (Figure 1). The combined solid state NMR (ssNMR), Raman spectroscopy and calorimetric investigations helped in determining the structural characteristics of the thermoset slabs. Their light concentration and optical efficiencies were determined with a properly designed setup[43] and compared to collectors made of PMMA thin films deposited on glasses with the same geometry of epoxy slabs.

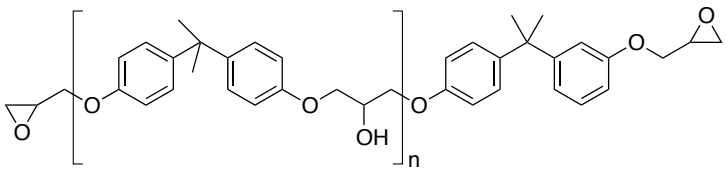

Bisphenol A diglycidyl ether (n = 1.2) (BADGE)

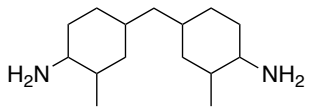

4,4'-methylenebis(2-methylcyclohexylamine)

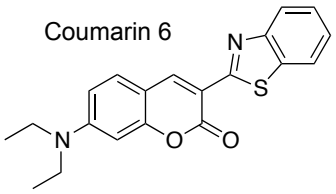

Coumarin 6

Lumogen Red F350

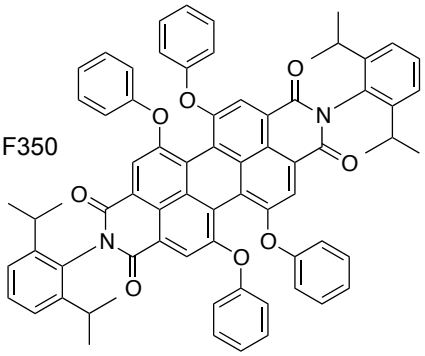

Figure 1. Epoxy resin precursors and fluorophores utilised in this study

2. Experimental section

2.1 Materials

Bisphenol A diglycidyl ether (BADGE) (Chemix Srl, Mw = 700 g/mol, d= 1.16 g/mL), Lumogen Red F350 (BASF), Coumarin 6 (>99%, Sigma Aldrich) were used as received. 4,4'-methylenebis(2-methylcyclohexylamine), mixture of isomers (Chemix Srl, d = 0.9 g/mL) was purified by distillation over KOH pellets at 130 °C and 0.3 mmHg. Poly(methyl methacrylate) (PMMA, Aldrich, Mw = 350,000 g/mol, acid number <1 mg KOH/g) was used as received.

2.2 Preparation of epoxy-based slabs

In a typical procedure, the appropriate amount of fluorophore was added to about 2 g of 4,4'-methylenebis(2-methylcyclohexylamine) in a Falcon™ conical centrifuge tube. The mixture was gently heated to allow dye dissolution in the diamine. Then, about 6.5 g of BADGE (about 10/3 by weight with respect to diamine) was added to the tube and the mixture homogenised with a mechanical stirrer at 80 °C for a few minutes. The homogeneous mixture was then centrifuged at 4500 rpm for 1h to remove air bubbles. The mixture was then casted at 110 °C in a mould (Figure S2) and cured at 110 °C for 4 hs. After cooling, the slab was separated by the mould and polished (Figure S3) to get the final size of 50x50x3 mm. The thickness was measured to be 3±0.1 mm.

2.3 Preparation of PMMA thin films

PMMA thin films were prepared by drop casting, that is pouring 0.8 mL $CHCl_3$ solution containing 30.5 mg of PMMA and the required content of Coumarin 6 (0.2–1.4 wt.%) on 50x50x3 mm optically pure glass slides (Edmund Optics Ltd BOROFLOAT window 50x50 TS). The glass slides were cleaned with 6 M HCl for 12 h, rinsed with water, acetone and isopropanol and dried for 8 h at 120 °C. Solvent evaporation was performed on a hot plate at about 30 °C and in a closed environment. The film thickness was measured by a Starrett micrometer to be 25±5 µm.

2.4 Apparatuses and methods

The thickness of the slabs was measured with a Starrett micrometer. Absorption spectra were recorded at room temperature on a Perkin–Elmer Lambda 650 spectrometer. Fluorescence spectra

were measured at room temperature on a Horiba Jobin–Yvon Fluorolog®-3 spectrofluorometer and equipped with a 450 W xenon arc lamp, double-grating excitation and single-grating emission monochromators. The fluorescence of epoxy and PMMA slabs were recorded by using the Solid-Sample Holder and collecting the front-face emission at 30°. FTIR-ATR spectra on solid samples were measured on Perkin Elmer GX with MIRacle TM ATR with a germanium crystal. Raman spectra were measured by using a XploRA ONE™ Raman confocal microscope at an excitation wavelength of 532 nm.

^{13}C CP/MAS (Cross Polarization/Magic Angle Spinning) spectra were recorded on a dual-channel Varian InfinityPlus 400 spectrometer, working at the Larmor frequencies of 400.03 MHz for proton and 100.67 MHz for carbon-13, equipped with a 7.5 mm CP/MAS probehead. The ^{1}H 90° pulse duration was 6 μs. The spectra were acquired under high-power decoupling and MAS conditions, using a MAS frequency of 4 kHz, a CP contact time of 500 μs, and accumulating 6000 transients with a relaxation delay between consecutive scans of 5 s. The ^{13}C chemical shifts were referenced to TMS as primary reference, while hexamethylbenzene was used as secondary reference. The spectra were recorded at 20 °C (± 0.1) using air as spinning gas. ^{1}H FID's (Free Induction Decay) were acquired on a spectrometer constituted by a Stelar PCNMR acquisition system coupled with a NiuMag permanent magnet, working at the ^{1}H Larmor frequency of 21 MHz. A solid-echo pulse sequence was applied under on-resonance conditions with an echo delay of 14 μs, a recycle delay of 1 s and accumulating 400 transients. The experiments were carried out at 25 °C (± 0.1).

Differential scanning calorimetry (DSC) measurements were performed with a Perkin-Elmer DSC Pyris equipped with a cooling system. The calibration was performed with Indium. Heating and cooling thermograms were carried out at a standard rate of 20 °C/min. Thermogravimetric scans were performed with a TA Instruments Q5000IR equipped with Agilent Resolution Pro version 5.2.0 software. Samples were heated from 30°C to 900 °C at 10 °C/min under nitrogen flow (25 mL/min).

2.5 Photocurrent measurements

A proper apparatus was build and composed by a plywood wooden box 15 x 15 x 30 cm with walls 1.5 cm thick. A removable cover hosting a housing for a solar lamp is present at the top. During the measurement a solar lamp TRUE-LIGHT® ESl E27 20W was used. Two 50x3 mm slits were carved out at 5 cm from the bottom of the box to exactly fit the collector systems (size 50x50x3 mm) so that the minimum amount of light would come out during the measurement conditions. On the outer side of the slit, a set of three 1x1 cm photodiodes (THORLABS FDS1010 Si photodiode, with an active area of 9.7x9.7 mm and high responsivity (A/W) in the spectral range of 400–1100 nm, figure S5) connected in parallel fashion was placed and coupled to a multimeter (KEITHLEY Mod. 2700) for photocurrent measuring. Notably, the active surface of the photodiods is larger than the LSC edge, anyway stray light was reduced by covering the analysed area with a black thick cloth. The photocurrent data were fitted by using the curve fitting routine in the program Igor Pro (Wavemetrics; Lake Oswego, OR).

2.6 Efficiency measurement using a PV-cell

A different set of collectors was prepared to measure the concentration efficiency attaching a Si-PV cell (IXYS SLMD121H08L mono solar cell 86x14 mm, with a solar cell efficiency of 22% and a fill factor > 70%, Figure S6) to one edge of the sample using silicone grease while the remaining edges were covered with an aluminum tape. The Si–based PV cell was masked with a dark tape to cover just the LSC edge (50x3 mm) aimed at reducing the stray light to negligible levels. These devices where then placed over a white poly(ethylene terephthalate) scattering sheet (Microcellular® MCPET reflective sheet, ERGA TAPES Srl) and placed about 20 cm under a solar lamp (TRUELIGHT® ESL E27 20W, with a correlated color temperature of 5500 K). The efficiency is reported as η_{opt}, which is the ratio between the short circuit current of the PV cell attached the collector edges under illumination of a light source (I_{LSC}) and the short circuit current of the bare cell put perpendicular to the light source (I_{SC}).

3. Results and discussion

3.1 Spectroscopic and calorimetric analyses of epoxy slabs

4,4'-methylenebis(2-methylcyclohexylamine) and Bisphenol A diglycidyl ether (BADGE) were used as the epoxy resin precursors. When fabricating the luminescent slabs, 60-150 ppm of the fluorophore was dissolved in the diamine and then BADGE was added (about 10/3 by weight with respect to diamine) under stirring at 80 °C for a few minutes. Air bubbles were removed by centrifugation prior curing at 110 °C for 4 hs. A final polishing step was required to get the 50x50x3 mm collector ready for structural and optical characterization. These conditions allowed to obtain highly homogeneous optically transparent epoxy slabs.

Epoxy slabs were initially characterized via spectroscopy aimed at determining their optical features and fluorophore compatibility within the thermoset matrix. Figure 2 shows the light transmitted in the visible range by the neat epoxy slab and the slabs containing 100 ppm of Coumarin 6 (Epoxy100 Coum) and Lumogen Red F350 (Epoxy100 Lumo), respectively.

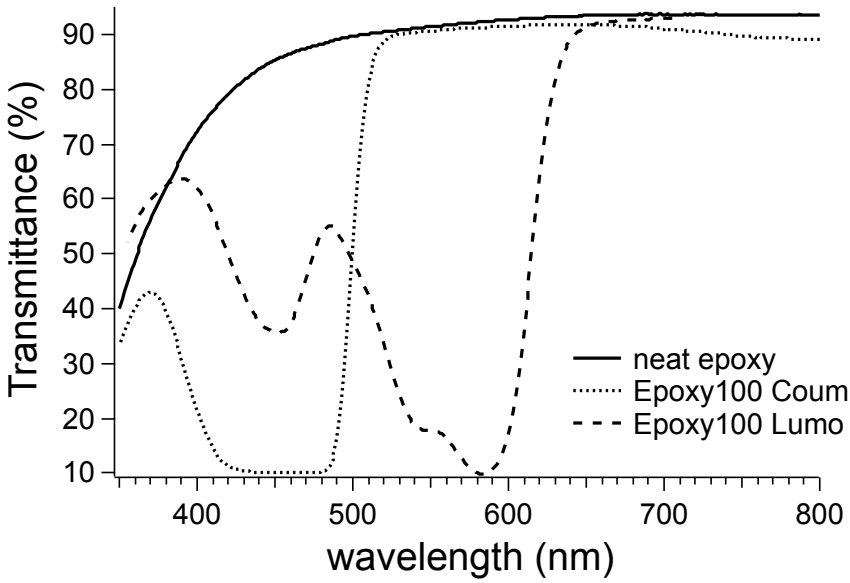

Figure 2. Visible transmittance spectra of 50x50x3 mm neat epoxy slab (straight line), the slabs containing 100 ppm of Coumarin 6 (Epoxy100 Coum, dotted line) and Lumogen Red F350 (Epoxy100 Lumo, dashed line), respectively.

The neat epoxy slab showed light transmittance around 90 % for most of the visible range, thus confirming the potential utility of this material in the fabrication of high performance luminescent collectors. A complete VIS-NIR spectrum of neat Epoxy was reported in Figure S1 as well as that

of a commercial PMMA matrix typically utilized for LSC applications. It is worth noting that epoxy preserves transparency along the entire NIR region, whereas PMMA shows significant light absorptions over 900-1000 nm.

Epoxy100 Coum and Epoxy100 Lumo displayed optical absorptions according to the characteristics of the corresponding fluorophores. Lumogen Red F350 absorbs at longer wavelengths (about 130 nm red-shifted) with respect to Coumarin 6, whereas signal saturation for Epoxy100 Coum possibly suggest a higher absorption extinction coefficient for the latter fluorophore.

Figure 3 shows the emission features of the epoxy slabs doped by the two fluorophores at different concentration. Epoxy slabs containing Coumarin 6 displayed a progressive and linear increase of the emission intensity peaked at 502 nm with fluorophore content (Figure 3a). No additional bands attributed to aggregates emerged with Coumarin 6 content, nor detectable fluorescence losses. The slab appeared optically clear and well homogeneous, i.e. indicating an excellent compatibility between the fluorophore and the thermosetting matrix. In contrast, epoxy slabs based on Lumogen Red F350 showed an emission centred at 615 nm (that is about 115 nm red-shifted compared to Coumarin 6, Figure 3b) that, however, appeared adversely affected by fluorophore concentration. The low fluorescence intensity that drops with dye content (Figure 3b, left inset), and the dull red colour of the slab, clearly suggest that compatibility issues between system components became apparent. Since solar harvesting in LSCs is favoured with high fluorophore content, epoxy slabs containing Lumogen Red F350 were disregarded in the successive studies.

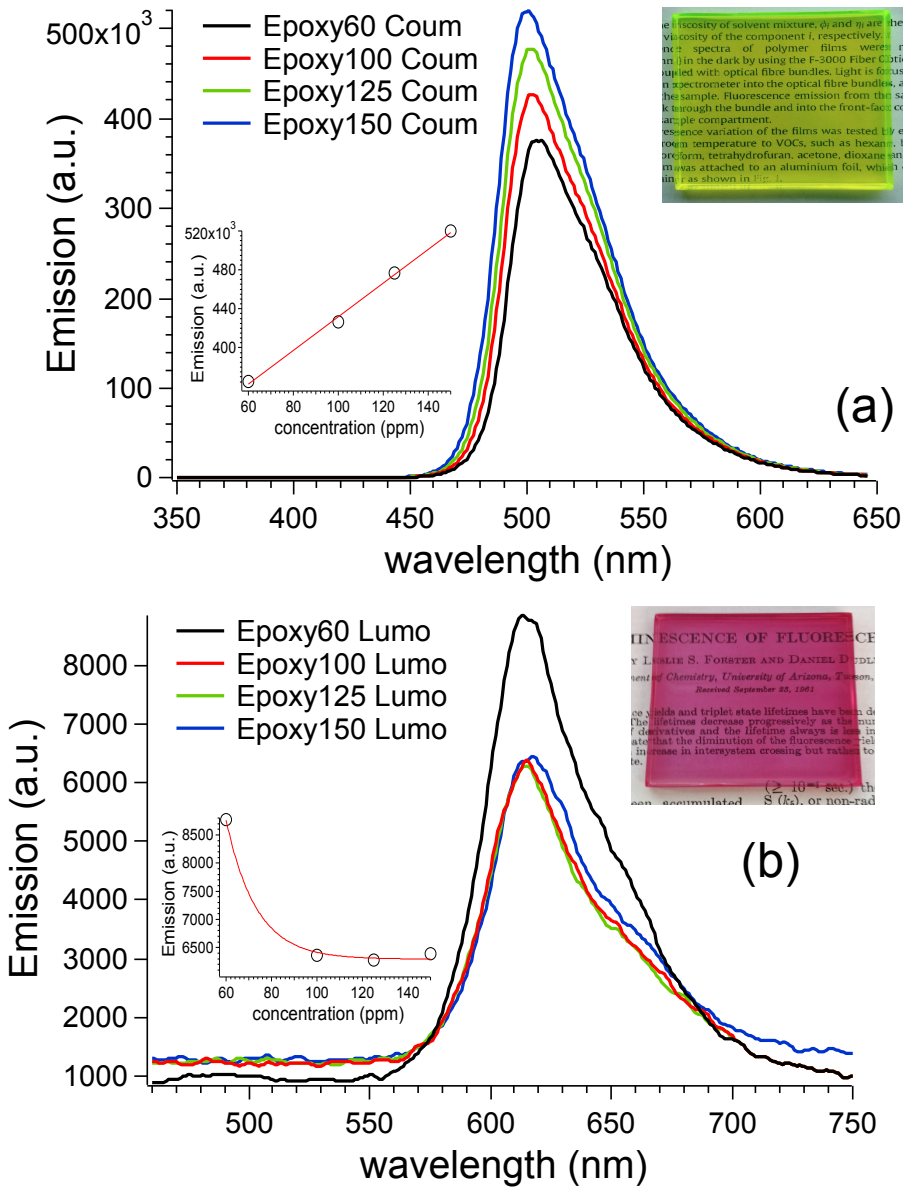

Figure 3. Fluorescence and images (insets) of epoxy slabs containing Coumarin 6 (a, $\lambda_{exc.}$ = 433 nm) and Lumogen Red F350 (b, $\lambda_{exc.}$ = 450 nm)

Neat epoxy slabs and those containing Coumarin 6 were then analysed in detail to investigate their structure and thermal behaviour after curing. FTIR spectra of BADGE, and epoxy slabs were compared looking at the intensities of the CH_2-O-CH bending of the epoxy group at about 915 cm^{-1} (Figure 4).[44] Data were also referred to a highly crosslinked epoxy slab obtained after curing the components according to the resin data sheet, i.e. four progressive annealing steps at 80 °C, 120 °C, 160 °C and 200 °C for 2 hours each. This procedure was not followed for the preparation of luminescent collectors since it promoted strong segregation of the fluorophore.

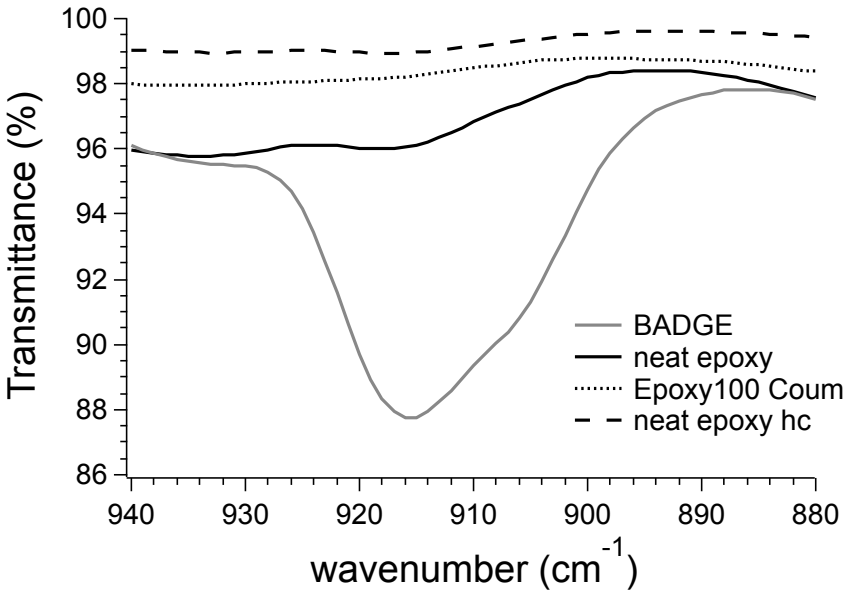

Figure 4. FTIR of BADGE, neat epoxy slab, neat epoxy slab highly crosslinked (neat epoxy hc) and epoxy slab containing 100 ppm of Coumarin 6

The neat epoxy slab displayed a residual absorption at 915 cm^{-1} due to the unreacted epoxy moieties, in contrast to the almost negligible contribution of the same slab after extensive curing at 200 °C. It is worth noting that the epoxy slab doped with 100 ppm of Coumarin 6 (Epoxy100 Coum) showed the same spectrum of the highly crosslinked system, thus suggesting that the fluorophore might act as a curing catalyst as analogously reported in literature for tertiary amines and Lewis bases.[45, 46] Quantitative analysis were performed taking into consideration the absorbance of the band at 915 cm^{-1} with respect to that of the 1,4-disubstituted aromatic ring stretching at 826 cm^{-1}. Notably, the extent of the epoxy conversion (α) were determined according to the equation 1:[44]

$$\alpha_{IR}\% = \left[1 - \frac{A_{915} \cdot A^0_{826}}{A_{826} \cdot A^0_{915}}\right] \cdot 100 \qquad \text{(eq. 1)}$$

where A^0_{826} and A^0_{915} are the absorbances of the epoxy peak for the uncrosslinked BADGE resin.

Table 1. Epoxy conversion values (α %) for the different epoxy slabs

Entry	α %
BADGE	0
Neat epoxy	54
Epoxy100 Coum	66
Neat epoxy hc	75

As expected, the highest conversion (75 %) was calculated for the highly crosslinked slab, whereas only 54% of epoxy groups were reacted following the experimental conditions that provided colourless epoxy slabs with negligible brittleness. Notably, the presence of 100 ppm of Coumarin 6 increased the epoxy conversion of about 20%.

In order to obtain information on the structural properties of the epoxy slabs, and in particular on the degree of epoxy group conversion, a ssNMR characterization was also performed, based on ^{13}C CP/MAS spectra and on the analysis of the on-resonance ^{1}H FID recorded under low-resolution conditions (^{1}H Larmor frequency of 21 MHz). The ssNMR experiments were carried out on the neat epoxy slab, the epoxy slab containing 150 ppm of Coumarin 6 (Epoxy150 Coum), and, as a reference system, on the highly crosslinked epoxy slab. ^{13}C CP/MAS spectra obtained for the three samples are shown in Figure 5, along with the signal assignment. The significant broadness of the spectral lines can be mainly ascribed to the complete amorphous character of these materials, for which the lack of conformational and long-range order is reflected in a distribution of ^{13}C chemical shift for each non-equivalent carbon. It is worth noticing that CP spectra cannot be considered as quantitative. Indeed, the efficiency of the magnetization transfer from the ^{1}H to the ^{13}C spin system depends on the strength of the ^{1}H-^{13}C dipolar couplings, so that signals from carbons with a larger number of attached protons and/or located in more rigid environment (i.e. involved in stronger ^{1}H-^{13}C dipolar couplings) are favoured. However, the spectra of the three samples here investigated were recorded under the same experimental conditions; moreover, as it will be further confirmed by ^{1}H FID analysis, it can be assumed that the dynamic properties of the system do not significantly

change: therefore, variations of signal intensities can be safely ascribed to changes of structural properties.

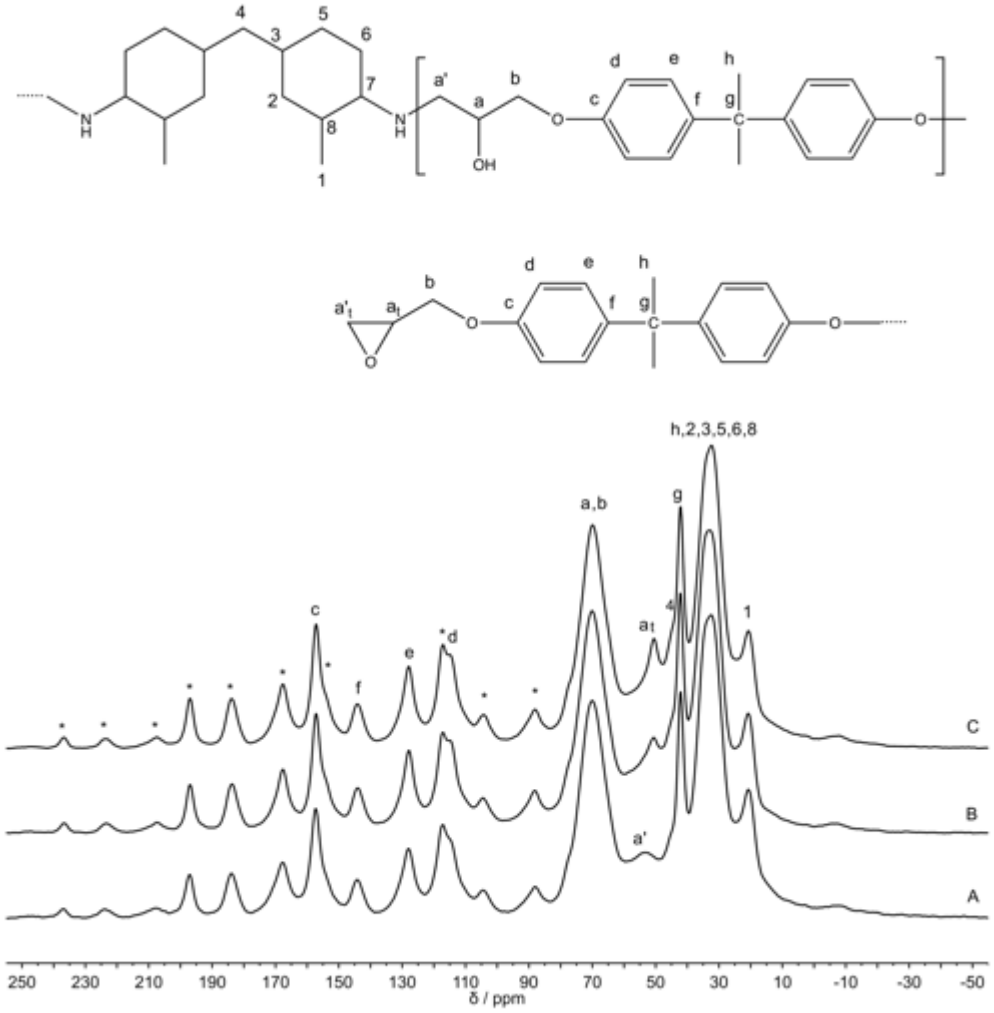

Figure 5. ^{13}C CP/MAS spectra of (A) the highly crosslinked epoxy slab, (B) the epoxy slab containing 150 ppm of Coumarin 6, and (C) the neat epoxy slab. The assignment of the different carbon signals is indicated. Spinning sidebands are marked with *.

All the spectra show the main signals of the epoxy resin aromatic and aliphatic carbons, as indicated in Figure 5, and are similar to each other apart from the 50-60 ppm spectral region, where significant differences among the samples can be observed. In particular, a signal at about 51 ppm is clearly observable in the spectra of the neat epoxy slab and of Epoxy150 Coum, but not in that of the highly crosslinked epoxy slab, which was ascribed to the CH carbon (a_t) of the terminal unreacted epoxide groups. It is interesting to notice that this signal significantly decreases in

passing from the neat epoxy slab to that containing 150 ppm of Coumarin 6, further indicating, in agreement with FTIR results, an increase of the epoxide group conversion in the presence of the fluorophore. In the spectrum of the highly crosslinked epoxy resin a quite broad signal at about 55 ppm is present, ascribable to the $\underline{C}H_2N$ carbon (a') formed after the reaction between the epoxide and the amino groups. This signal is not clearly observable in the spectra of the neat epoxy slab and of Epoxy150 Coum, characterized by a lower degree of crosslinking, probably due to its intrinsic lower intensity in these samples combined with the scarce spectral resolution. The analysis of the ^1H FID recorded under on resonance conditions could also be useful to obtain information on the degree of crosslinking. In this analysis, the experimental FID's are fitted by means of a linear combination of functions, chosen among Gaussian, exponential, Abragamian, Weibullian and Pake functions, each characterized by a different value of ^1H T_2 relaxation time.[47] Since in the solid state, ^1H T_2 monotonically increases with the degree of mobility, due to the motional averaging of the strong ^1H-^1H dipolar couplings, this analysis allows different polymeric domains to be distinguished on the basis of their degree of mobility. Furthermore the weight of each function in the linear combination is proportional to the fractional population of protons in the domain, providing quantitative information. The ^1H FID's of the three samples here investigated were well reproduced by means of a linear combination of a Gaussian function characterized by a very short T_2 of about 16 μs, which accounts for almost the 90 % of the protons, and an exponential function with a slightly longer T_2 of about 30-50 μs. The results of the ^1H FID analysis are reported in Table 2, while in Figure S7, as an example, the experimental ^1H FID obtained for the sample Epoxy150 Coum is shown together with the best fitting function and each component of the linear combination. The short values of ^1H T_2 characterizing both the Gaussian and the exponential functions indicate that the epoxy resin chains experience a very low degree of mobility in all the samples. The exponential function can be ascribed to epoxy resin segments located in more mobile environment, but its assignment to specific groups is not possible on the basis of the sole weight in the linear combination (8-14 %). However, it is reasonable that terminal unreacted epoxide groups,

characterized by a slightly higher degree of mobility, contribute to this component. To this respect it is interesting to note that the weight of this exponential component is slightly smaller for the highly crosslinked epoxy slab and the epoxy slab containing 150 ppm of Coumarin 6, for which a higher degree of epoxide group conversion was already highlighted by FTIR and ^{13}C CP/MAS ssNMR spectra.

Table 2. Results of the fitting of the experimental ^{1}H FID obtained for the neat epoxy slab (Neat epoxy), the epoxy slab containing 150 ppm of Coumarin 6 (Epoxy150 Coum), and the highly crosslinked epoxy slab (Neat epoxy hc). A linear combination of a Gaussian (GAU) and an exponential (EXP) function was used in all cases to fit the experimental FID. The weights in the linear combination (w %) and the ^{1}H T_2 (μs) values for each component are reported.

	Neat epoxy hc	**Epoxy150 Coum**	**Neat epoxy**
GAU: T_2 (μs)	15.6	15.6	15.6
w (%)	91.8	90.8	86.4
EXP: T_2 (μs)	47.5	40.8	28
w (%)	8.2	9.2	13.6

The thermal behaviour of the prepared epoxy slabs was determined by differential scanning calorimetry (DSC, Figure S8) and confirmed the results acquired by spectroscopy. The neat epoxy slab showed a glass transition temperature (Tg) of 112 °C, which is a typical value of partially cured resins with negligible brittleness.[48] Tg increased to 132 °C and 150 °C for epoxy100 Coum and neat epoxy hc slabs, respectively, thus confirming that the curing process was favoured at higher temperature and promoted by the presence of Coumarin 6.

Epoxy groups conversion was also evaluated by means of Raman spectroscopy by monitoring Raman bands corresponding to epoxide vibration in the range of 1230 cm^{-1} and 1280 cm^{-1} (Figure 6). Notably, the intensity of the peak at 1254 cm^{-1}, which is attributed to the breathing of the epoxide ring, is dependent on the concentration of epoxide groups in the resin mixture.[49]

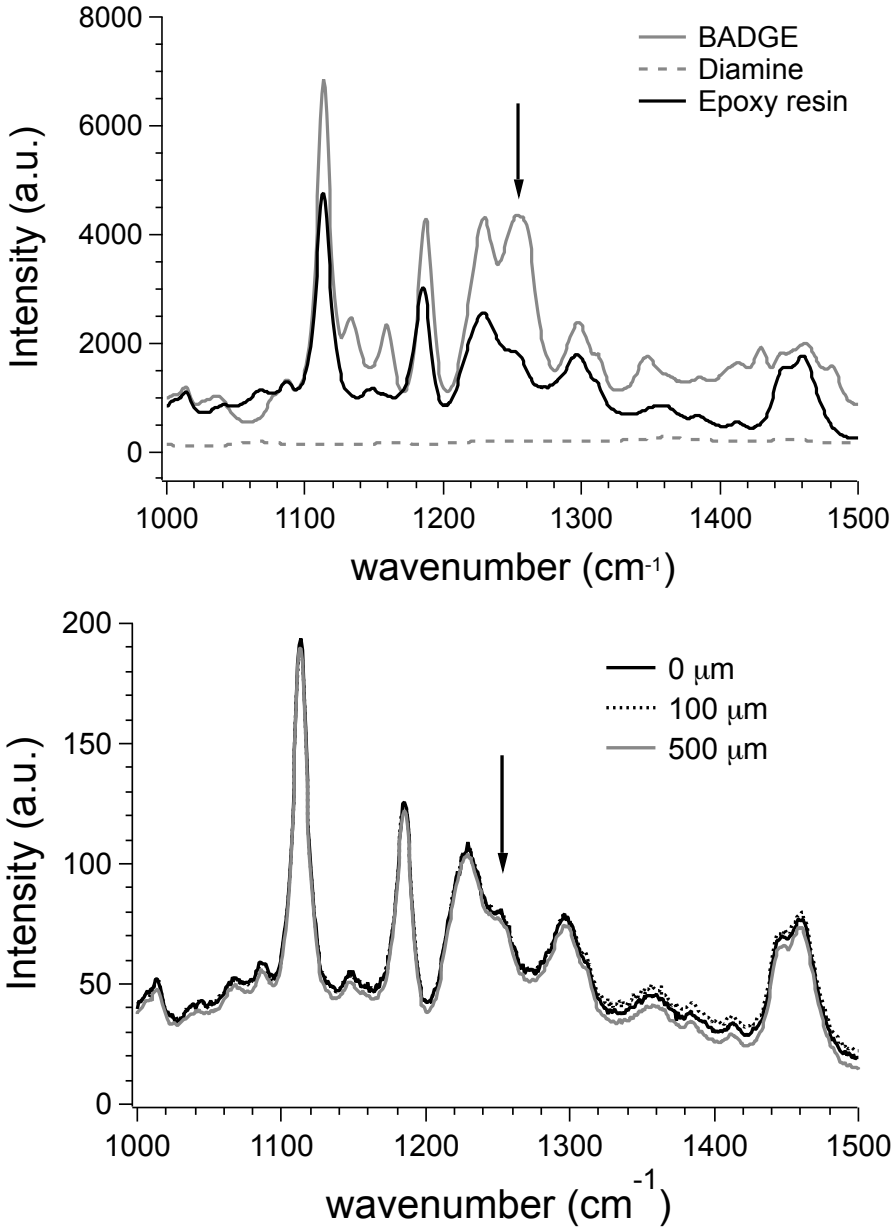

Figure 6. Raman microscopy spectra of (a) the neat epoxy slab and reactants and (b) of epoxy slab at different z-scan depths ($\lambda_{exc.}$ = 532 nm).

In Figure 6a, the Raman spectrum of the epoxy slab was compared to those of reactants, i.e. BADGE and the 4,4'-methylenebis(2-methylcyclohexylamine) (diamine). It was observed that the 1254 cm^{-1} epoxide ring vibration decreased in intensity but did not completely disappear according to the results obtained by FTIR investigations. Nevertheless, Raman scattering intensity was identical at different slab depths, thus indicating that the curing process homogeneously occurred within the epoxy slab (Figure 6b).

3.2 Photocurrent measurements and data analysis of epoxy and PMMA fluorescent collectors

Photocurrent measurements were accomplished with a home-built apparatus (see experimental part) by using a set of three 1x1 cm photodiodes assembled in parallel fashion. Photodiodes are ideal for measuring light sources in fluorescent collectors by converting the optical power to an electrical current, allowing for a fast, precise and reproducible response even with different sets of samples. This approach was used to study the best working conditions for different epoxy slabs doped with Coumarin 6 since the response curves of the photodiodes and the utilized PV module do not differ significantly. Notably, the active surface of the photodiods is larger than the LSC edge, anyway stray light was reduced by covering the analysed area with a black thick cloth. Since photodiods measurements are aimed at determining relative variations of optical parameters between samples and not absolute values, data are considered meaningful since stray light affect all measurements in the same way. Photocurrents produced by luminescent epoxy slabs were reported in Figure 7 and compared to that generated by Coumarin 6 dispersed in poly(methyl methacrylate) (PMMA) thin films (25±5 μm), that is the reference polymer matrix for luminescent collectors. For thin PMMA films, a comparable range of Coumarin 6 concentration was selected as also suggested by earlier investigations with different classes of fluorophores.[43, 50, 51] In order to get comparable data, PMMA/Coumarin 6 films were attached on 50x50x3 mm optically pure glass substrate, i.e. characterized by the same aspect ratio and geometry of the Epoxy/Coumarin 6 slabs.

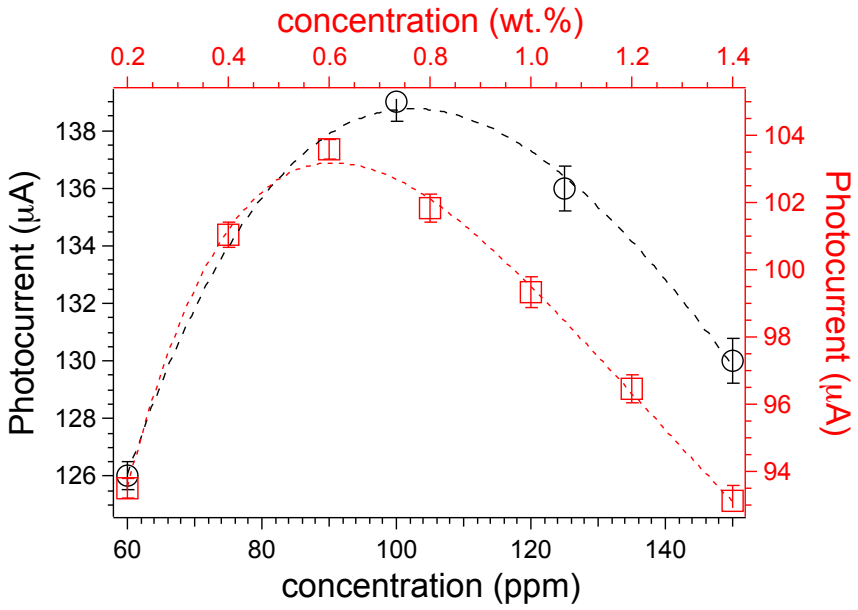

Figure 7. Photocurrent variation of 5x5x0.3 cm Epoxy/Coumarin 6 (black open circles) slabs and PMMA/Coumarin 6 thin films (red open squares). The curves were fitted with eq. 2 with parameters listed in Table 3.

The current intensities for both Epoxy/ and PMMA/Coumarin 6 collectors were found to increase up to a certain content of fluorophore, above which a decline became apparent due to the prevailing dissipative phenomena of the emission response.

Notably, both photocurrent curves fitted quite well according to eq. 2:

$$\eta_{opt} = \varepsilon' \cdot c \cdot e^{-\mu_{opt} \cdot c} + D \qquad \text{(eq. 2)}$$

where η_{opt} is a term proportional to the current generated by photodiods, c is the concentration of the dye in wt.%, and ε' and μ_{opt} are two empirical constants defined as:

$$\varepsilon' \propto h \cdot e^{-\bar{l}} \qquad \text{(eq. 3)}$$

$$\mu_{opt} \propto \mu''(QY, p) \cdot \bar{l} \qquad \text{(eq. 4)}$$

where h is the thickness of the thin film, $\bar{l}$ is the mean path length of the radiation in the optical system and μ'' is a term depending on both QY and the probability of fluorescence re-absorption (p), being greater at high p and low QY. D is an empirical constant added since even an empty system of transparent material (c = 0) is capable of trapping some light by means of surface and bulk defects due to scattering phenomena. Eq. 2 was inspired by the work of Goezberger[52] who

proposed in 1977 an effective method to evaluate the collectors efficiency. Both ε' and μ_{opt} must be considered as completely empirical since even the most accurate estimations require strong approximations. Nevertheless, the determination of how they affect the final η_{opt} is straightforward for determining the performances of luminescent collectors. Notably, ε' is a coefficient related to the absorption properties of the dye/polymer system, whereas μ_{opt} combines all the fluorescence quenching mechanisms due to the dye. An optimal dye/polymer system should therefore present a high ε' and a small μ_{opt} so that the maximum efficiency is shifted to higher concentrations and the curve steadily rises under the influence of the linear part (eq. 2). A complete and exhaustive determination of eq. 2 was recently reported in literature by our group.[43] The fitting parameters of photocurrents were reported in table 2.

Table 3. Fitting parameters of the photocurrent data measured for Coumarin 6-based luminescent collectors

Entry	ε'	μ_{opt}	D
Epoxy Coumarin 6	2.97±0.45	0.010±0.002	70±1
PMMA Coumarin 6	3.00±0.03	0.026±0.001	76±1

The fitting parameters of Epoxy/Coumarin 6 slabs were found to be similar of those of PMMA/Coumarin 6 thin films, even if worthwhile differences are present. Notably, identical values for ε' and smaller μ_{opt} were obtained for the former collectors. On the contrary, D values resulted to be quite similar for all the systems since the contribution of non–fluorescent trapping is mostly the same for systems with the same geometry. Being ε' related to the light absorption properties of the material at low fluorophore content, identical ε' values in both polymer matrices were expected. In contrast, higher μ_{opt} value calculated for PMMA/Coumarin 6 suggested that larger dissipative phenomena occurred in PMMA with fluorophore content that adversely affected fluorescence concentration.

Epoxy and PMMA luminescent slabs were then analysed by using a Si-based PV cell attached to one edge of the collector, as described in the experimental section. As reported, the stray light was reduced to negligible levels by masking the Si–based PV cell with a dark tape to cover just the LSC

edge. The optical efficiency η_{opt} (Table 4) was evaluated from the concentration factor C, which is the ratio between the short circuit current measured in the case of the cell over the collector edge (I_C) and short circuit current of the bare cell when perpendicular to the light source (I_{SC}) (eq. 4):

$$\eta_{opt} = \frac{I_C}{I_{SC} \cdot G} \qquad \text{(eq. 4)}$$

where G is the geometrical factor (in our case, G = 16.6), which is the ratio between the area exposed to the light source and the collecting area.

Table 4. Concentration factors (C) and optical efficiencies (η_{opt}) calculated for Epoxy/ and PMMA/Coumarin 6 LSCs

Entry	C	η_{opt} (%)
Epoxy Coumarin 6	1.23±0.02	7.4
PMMA Coumarin 6	1.13±0.01	6.7

The maximum η_{opt} calculated for the Epoxy/Coumarin 6 was found higher than that gathered from PMMA collectors with the same geometrical factor, possibly due to the higher fluorophore compatibility in the epoxy matrix. This phenomenon limits the adverse dissipative disexcitation processes, thus increasing concentration efficiency of about 10%, and enabling the use of epoxy resins for the preparation of efficient luminescent collectors. Although such difference could be also addressed to the different fluorescence self-absorption occurring in the PMMA film, Fusco et al demonstrated that that the maximum conversion efficiencies found for the slab and thin film are identical, though they are obtained for different dye concentrations.[53]

As far as final application in LSC is concerned, experiments are being made to determine the photostability of the epoxy-based system with time. Preliminarily results evidenced a loss of optical efficiency of about 25% after sun exposure during summertime (from June to September) in Pisa (Italy). This drop in optical performances was mostly addressed to fluorophore photodegradation[54] (Figure S9) since epoxy degradation under photolytic conditions would be possibly prevented by the presence of the UV-absorbing fluorophore (see also the note below Figure S10). Nevertheless, we are confident that the introduction of triplet-state quenchers or redox-

active compounds[55] in the final system recipe would contribute to the overall photostability of the luminescent collectors during continuous sun irradiation.

Conclusions

We have demonstrated that a low cost and optically transparent epoxy resin can be effectively used to prepare accessible and effective fluorescent collectors. The slabs were prepared by carefully mixing from 60 to 150 ppm of the fluorophore with Bisphenol A diglycidyl ether and 4,4'-methylenebis(2-methylcyclohexylamine) as curing agent. Coumarin 6 was selected as highly emissive fluorophore being well miscible in the thermoset matrix in the range of concentration investigated. Spectroscopic and calorimetric investigations revealed that the curing process at 110 °C for 4 hs provided highly homogeneous epoxy slabs whose crosslinking degree was affected by the presence of Coumarin 6 that acted as a curing agent. Photocurrent measurements and data analysis of epoxy slabs yielded maximum optical efficiencies (η_{opt}) of 7.4% that were found higher than that gathered from PMMA collectors with the same geometry. Overall, considering the easy preparation, low cost, optical transparency, and concentration performances, all findings consistently support the effective use of epoxy resins as bulk thermosetting materials for fluorescent collectors in PV applications.

Acknowledgements

The research leading to these results has received funding from MIUR-FIRB (RBFR122HFZ) and in part from the Università di Pisa under PRA 2015 (project No. 2015_0038). Horiba Italia SRL is kindly acknowledged for the help in Raman measurements.

References

[1] Armaroli N, Balzani V. Solar Electricity and Solar Fuels: Status and Perspectives in the Context of the Energy Transition. Chemistry – A European Journal 2016:22(1):32-57.
[2] Sawin JL. Renewables Global Status Report. Paris: Renewable Energy Policy Network for the 21th Century, 2014.
[3] van Sark WGJHM. Luminescent solar concentrators - A low cost photovoltaics alternative. Renewable Energy 2013:49(0):207-210.
[4] BIPV Technologies and Markets 2015-2022. Dublin, Ireland, 2015.

[5] Debije MG, Verbunt PPC. Thirty Years of Luminescent Solar Concentrator Research: Solar Energy for the Built Environment. Advanced Energy Materials 2012:2(1):12-35.
[6] Benjamin WE, Veit DR, Perkins MJ, Bain E, Scharnhorst K, McDowall S, Patrick DL, Gilbertson JD. Sterically Engineered Perylene Dyes for High Efficiency Oriented Fluorophore Luminescent Solar Concentrators. Chemistry of Materials 2014:26(3):1291-1293.
[7] Currie MJ, Mapel JK, Heidel TD, Goffri S, Baldo MA. High-Efficiency Organic Solar Concentrators for Photovoltaics. Science 2008:321(5886):226-228.
[8] Desmet L, Ras AJM, de Boer DKG, Debije MG. Monocrystalline silicon photovoltaic luminescent solar concentrator with 4.2% power conversion efficiency. Opt Lett 2012:37(15):3087-3089.
[9] Griffini G, Levi M, Turri S. Thin-film luminescent solar concentrators: A device study towards rational design. Renewable Energy 2015:78:288-294.
[10] Meinardi F, Colombo A, Velizhanin KA, Simonutti R, Lorenzon M, Beverina L, Viswanatha R, Klimov VI, Brovelli S. Large-area luminescent solar concentrators based on /`Stokes-shift-engineered/' nanocrystals in a mass-polymerized PMMA matrix. Nat Photon 2014:8(5):392-399.
[11] Meinardi F, McDaniel H, Carulli F, Colombo A, Velizhanin KA, Makarov NS, Simonutti R, Klimov VI, Brovelli S. Highly efficient large-area colourless luminescent solar concentrators using heavy-metal-free colloidal quantum dots. Nat Nano 2015:10(10):878-885.
[12] Sanguineti A, Sassi M, Turrisi R, Ruffo R, Vaccaro G, Meinardi F, Beverina L. High Stokes shift perylene dyes for luminescent solar concentrators. Chemical Communications 2013:49(16):1618-1620.
[13] Zhao Y, Meek GA, Levine BG, Lunt RR. Near-Infrared Harvesting Transparent Luminescent Solar Concentrators. Advanced Optical Materials 2014:2(7):606-611.
[14] El Mouedden Y, Ding B, Song Q, Li G, Alameh K. Encapsulation of tandem organic luminescence solar concentrator with optically transparent triple layers of SiO2/epoxy/SiO2. IEEE J Sel Top Quantum Electron 2016:22(1):4100306/4100301-4100306/4100306.
[15] Li Y, Olsen J, Nunez-Ortega K, Dong W-J. A structurally modified perylene dye for efficient luminescent solar concentrators. Sol Energy 2016:136:668-674.
[16] Nikolaidou K, Sarang S, Hoffman C, Mendewala B, Ishihara H, Lu JQ, Ilan B, Tung V, Ghosh S. Hybrid Perovskite Thin Films as Highly Efficient Luminescent Solar Concentrators. Advanced Optical Materials 2016:4(12):2126-2132.
[17] Zhao H, Benetti D, Jin L, Zhou Y, Rosei F, Vomiero A. Solar Concentrators: Absorption Enhancement in "Giant" Core/Alloyed-Shell Quantum Dots for Luminescent Solar Concentrator (Small 38/2016). Small 2016:12(38):5368.
[18] Banal JL, Zhang B, Jones DJ, Ghiggino KP, Wong WWH. Emissive Molecular Aggregates and Energy Migration in Luminescent Solar Concentrators. Acc Chem Res 2017:50(1):49-57.
[19] Bailey ST, Lokey GE, Hanes MS, Shearer JDM, McLafferty JB, Beaumont GT, Baseler TT, Layhue JM, Broussard DR, Zhang Y-Z, Wittmershaus BP. Optimized excitation energy transfer in a three-dye luminescent solar concentrator. Solar Energy Materials and Solar Cells 2007:91(1):67-75.
[20] Flores Daorta S, Proto A, Fusco R, Claudio Andreani L, Liscidini M. Cascade luminescent solar concentrators. Applied Physics Letters 2014:104(15):-.
[21] Correia SFH, Lima PP, Pecoraro E, Ribeiro SJL, Andre PS, Ferreira RAS, Carlos LD. Scale up the collection area of luminescent solar concentrators towards metre-length flexible waveguiding photovoltaics. Progress in Photovoltaics 2016:24(9):1178-1193.
[22] Kanellis M, de Jong MM, Slooff L, Debije MG. The solar noise barrier project: 1. Effect of incident light orientation on the performance of a large-scale luminescent solar concentrator noise barrier. Renewable Energy 2017:103:647-652.
[23] Tummeltshammer C, Portnoi M, Mitchell SA, Lee A-T, Kenyon AJ, Tabor AB, Papakonstantinou I. On the ability of Forster resonance energy transfer to enhance luminescent solar concentrator efficiency. Nano Energy 2017:32:263-270.
[24] Slooff LH, Bende EE, Burgers AR, Budel T, Pravettoni M, Kenny RP, Dunlop ED, Büchtemann A. A luminescent solar concentrator with 7.1% power conversion efficiency. physica status solidi (RRL) – Rapid Research Letters 2008:2(6):257-259.
[25] Silikas N, Al-Kheraif A, Watts DC. Influence of P/L ratio and peroxide/amine concentrations on shrinkage-strain kinetics during setting of PMMA/MMA biomaterial formulations. Biomaterials 2005:26(2):197-204.
[26] Toshikuni K. Absorption Losses of Low Loss Plastic Optical Fibers. Japanese Journal of Applied Physics 1985:24(12R):1661.

[27] Global Industry Analysts I. Epoxy Resins: A Global Strategic Business Report. In: Global Industry Analysts I, editor, 2016.
[28] Jin F-L, Li X, Park S-J. Synthesis and application of epoxy resins: A review. Journal of Industrial and Engineering Chemistry 2015:29:1-11.
[29] Partanen A, Harju A, Mutanen J, Lajunen H, Pakkanen T, Kuittinen M. Luminescent optical epoxies for solar concentrators. 2014. p. 91750S-91750S-91756.
[30] Wan J, Gan B, Li C, Molina-Aldareguia J, Kalali EN, Wang X, Wang D-Y. A sustainable, eugenol-derived epoxy resin with high biobased content, modulus, hardness and low flammability: Synthesis, curing kinetics and structure–property relationship. Chemical Engineering Journal 2016:284:1080-1093.
[31] Qin J, Liu H, Zhang P, Wolcott M, Zhang J. Use of eugenol and rosin as feedstocks for biobased epoxy resins and study of curing and performance properties. Polymer International 2014:63(4):760-765.
[32] Wang L, Wong CP. Syntheses and characterizations of thermally reworkable epoxy resins. Part I. Journal of Polymer Science Part A: Polymer Chemistry 1999:37(15):2991-3001.
[33] Araya-Hermosilla R, Lima GMR, Raffa P, Fortunato G, Pucci A, Flores ME, Moreno-Villoslada I, Broekhuis AA, Picchioni F. Intrinsic self-healing thermoset through covalent and hydrogen bonding interactions. European Polymer Journal 2016:81:186-197.
[34] Yang Y, Li Y-Q, Fu S-Y, Xiao H-M. Transparent and Light-Emitting Epoxy Nanocomposites Containing ZnO Quantum Dots as Encapsulating Materials for Solid State Lighting. The Journal of Physical Chemistry C 2008:112(28):10553-10558.
[35] Tang L, Whalen J, Schutte G, Weder C. Stimuli-Responsive Epoxy Coatings. ACS Applied Materials & Interfaces 2009:1(3):688-696.
[36] Huang J-C, Chu Y-P, Wei M, Deanin RD. Comparison of epoxy resins for applications in light-emitting diodes. Advances in Polymer Technology 2004:23(4):298-306.
[37] Bauer RS. Application of Epoxy Resins in Electronics A2 - Wong, C.P. San Diego: Academic Press, 1993. p. 287-331.
[38] Altan Bozdemir O, Erbas-Cakmak S, Ekiz OO, Dana A, Akkaya EU. Towards Unimolecular Luminescent Solar Concentrators: Bodipy-Based Dendritic Energy-Transfer Cascade with Panchromatic Absorption and Monochromatized Emission. Angew Chem, Int Ed 2011:50(46):10907-10912, S10907/10901-S10907/10948.
[39] Bastianini M, Vivani R, Nocchetti M, Costenaro D, Bisio C, Oswald F, Meyer TB, Marchese L. Effect of iodine intercalation in nanosized layered double hydroxides for the preparation of quasi-solid electrolyte in DSSC devices. Solar Energy 2014:107:692-699.
[40] Eronen A, Harju A, Mutanen J, Lajunen H, Suvanto M, Pakkanen T, Kuittinen M. Micropatterned luminescent optical epoxies. Opt Express 2015:23(26):33419-33425.
[41] Tummeltshammer C, Taylor A, Kenyon AJ, Papakonstantinou I. Losses in luminescent solar concentrators unveiled. Solar Energy Materials and Solar Cells 2016:144:40-47.
[42] Carlotti M, Ruggeri G, Bellina F, Pucci A. Enhancing optical efficiency of thin-film luminescent solar concentrators by combining energy transfer and stacked design. Journal of Luminescence 2016:171:215-220.
[43] Carlotti M, Panniello A, Fanizza E, Pucci A. A Fast and Effective Procedure for the Optical Efficiency Determination of Luminescent Solar Concentrators. Solar Energy 2015:119:452-460.
[44] Nikolic G, Zlatkovic S, Cakic M, Cakic S, Lacnjevac C, Rajic Z. Fast Fourier Transform IR Characterization of Epoxy GY Systems Crosslinked with Aliphatic and Cycloaliphatic EH Polyamine Adducts. Sensors 2010:10(1).
[45] Lin YG, Galy J, Sautereau H, Pascault JP. Mechanism of reaction and processing properties relationships for dicyandiamide cured epoxy resins. Crosslinked Epoxies, Proc Discuss Conf, 9th 1987:147-168.
[46] Pascault J-P, Williams RJJ. General Concepts about Epoxy Polymers. Wiley-VCH Verlag GmbH & Co. KGaA, 2010. p. 1-12.
[47] Hansen EW, Kristiansen PE, Pedersen B. Crystallinity of Polyethylene Derived from Solid-State Proton NMR Free Induction Decay. The Journal of Physical Chemistry B 1998:102(28):5444-5450.
[48] Ellis B, Found MS, Bell JR. Effects of cure treatment on glass transition temperatures for a BADGE–DDM epoxy resin. Journal of Applied Polymer Science 1996:59(10):1493-1505.
[49] Lyon RE, Chike KE, Angel SM. In situ cure monitoring of epoxy resins using fiber-optic Raman spectroscopy. Journal of Applied Polymer Science 1994:53(13):1805-1812.

[50] Bellina F, Manzini C, Marianetti G, Pezzetta C, Fanizza E, Lessi M, Minei P, Barone V, Pucci A. Colourless p-phenylene-spaced bis-azoles for luminescent concentrators. Dyes and Pigments 2016:134:118-128.
[51] Pucci A, Pavone M, Minei P, Munoz-Garcia AB, Fanizza E, Cimino P, Rodriguez A. Cost-effective Solar Concentrators based on Red Fluorescent Zn(II)-Salicylaldiminato Complex. RSC Advances 2016:6:17474-17482.
[52] Goetzberger A, Greube W. Solar energy conversion with fluorescent collectors. Appl Phys 1977:14(2):123-139.
[53] Daorta SF, Liscidini M, Andreani LC, Scudo P, Fusco R. THEORETICAL STUDY OF MULTILAYER LUMINESCENT SOLAR CONCENTRATORS USING A MONTE CARLO APPROACH. Hamburg, 2011.
[54] Jones G, Bergmark WR, Jackson WR. Products of photodegradation for coumarin laser dyes. Optics Communications 1984:50(5):320-323.
[55] Zheng Q, Juette MF, Jockusch S, Wasserman MR, Zhou Z, Altman RB, Blanchard SC. Ultra-stable organic fluorophores for single-molecule research. Chemical Society Reviews 2014:43(4):1044-1056.